

Alma Mater Studiorum Università di Bologna
Archivio istituzionale della ricerca

Photostability assessment of natural pyrethrins using halloysite nanotube carrier system

This is the final peer-reviewed author's accepted manuscript (postprint) of the following publication:

Published Version:

M. Massaro, S.P. (2022). Photostability assessment of natural pyrethrins using halloysite nanotube carrier system. APPLIED CLAY SCIENCE, 230, 106719-106729 [10.1016/j.clay.2022.106719].

Availability:

This version is available at: <https://hdl.handle.net/11585/895747> since: 2023-09-06

Published:

DOI: <http://doi.org/10.1016/j.clay.2022.106719>

Terms of use:

Some rights reserved. The terms and conditions for the reuse of this version of the manuscript are specified in the publishing policy. For all terms of use and more information see the publisher's website.

This item was downloaded from IRIS Università di Bologna (<https://cris.unibo.it/>).
When citing, please refer to the published version.

(Article begins on next page)

Photostability assessment of natural pyrethrins using halloysite nanotube carrier system

M. Massaro,^a S. Pieraccini,^b S. Guernelli,^{b*} M. L. Dindo,^c S. Francati,^c L.F. Liotta,^d G.C. Colletti,^a
S. Masiero,^b and S. Riela^{a*}

^aDipartimento di Scienze e Tecnologie Biologiche Chimiche e Farmaceutiche (STEBICEF),
Università degli Studi di Palermo, Parco d'Orleans II, Ed. 17, 90128 Palermo, Italy. Email:
serena.riela@unipa.it

^bDipartimento di Chimica “G. Ciamician”, Università degli Studi di Bologna, Via S. Giacomo 11,
40126 Bologna, Italy. E-mail: susanna.guernelli@unibo.it

^cDipartimento di Scienze e Tecnologie Agro-Alimentari, Università degli Studi di Bologna, Viale
Fanin 42, 40127 Bologna, Italy.

^dIstituto per lo Studio dei Materiali Nanostrutturati (ISMN)-CNR, Via Ugo La Malfa 153, Palermo
90146, Italy.

1 Abstract

2 Natural pyrethrins are one of the most used pesticides and insect repellents employed for domestic
3 or agronomic use. However, they are highly hydrophobic and suffer from insolubility in water
4 media and ready decomposition by photochemical, and oxidative actions. These aspects hamper
5 their long-term storage and applicability. Herein, we report the synthesis and characterization of a
6 nanomaterial based on the loading of pyrethrum extract (PE) into natural, low-cost, and eco-
7 compatible halloysite nanotubes (Hal). The Hal/PE nanomaterial was thoroughly characterized, and
8 the morphology was imaged by TEM and SEM investigations.

9 Release experiments showed a slow release of pyrethrins from the carrier, and photodegradation
10 studies, both in solution and in a solid state, highlighted that the pyrethrum extract in the Hal/PE
11 nanomaterial showed high stability to UV irradiation, as proved by UPLC-ESI-MS, UV-*vis*, and
12 circular dichroism measurements.

13 Furthermore, to check if the obtained nanomaterial possesses the insecticidal activity of the
14 pyrethrum, *in vivo* tests on two model insects, *Galleria mellonella* and *Tenebrio molitor*, were
15 performed. The pyrethrins loaded onto Hal showed the same activity as standard pyrethrins, at half
16 dose compared to them.

17 Keywords: pyrethrins, halloysite, photoprotection, nanopesticides.

18

1. Introduction

Agriculture is the major source of food in the world. Nowadays, environmental pollution, climate change, and agricultural crop pests jeopardize plant cultivation hampering overall food production (Gomez-Zavaglia et al., 2020; Praveen and Sharma, 2019). In this context, commonly used pesticides are more and more inefficient due to the occurrence of resistance phenomena (Bombo et al., 2019; Martin, 2004).

Plant extracts or their bioactive compounds are increasingly used as alternatives to synthetic pesticides for sustainable pest control, with less impact on the environment and human health.

Pyrethrum, a natural extract of *Tanacetum cinerariifolium* (Trevir.) Sch.Bip., represents one of the most commonly used pesticides and insect repellents, both for agricultural and domestic purposes (Kalaitzaki et al., 2015; Markham et al., 2021; Papanikolaou et al., 2018). The extract constituents, responsible of its insecticidal and repellent activity are six esters (pyrethrin I, pyrethrin II, cinerin I, cinerin II, jasmolin I and jasmolin II), commonly known as pyrethrins. The biological activities of the pyrethrum constituents depend on the structures and stereochemical characteristics of both the acid and alcohol components. Among the six components, pyrethrin I and II are the most dominant and active (Jeran et al., 2021).

Unfortunately, although the pyrethrum extract possesses a high insecticidal action and low residual power, it suffers from ready decomposition by thermal, photochemical, and oxidative actions which hamper its long-term storage and applicability (Zhang et al., 2019). In addition, due to its hydrophobic chemical composition, organic solvents are necessary in its formulations which contribute to environmental pollution.

In recent years, the use of nanomaterials as a carrier for pesticides (Kah et al., 2018; Zhong et al., 2017), that can take over organic solvents in their formulations, has offered some advantages in terms of enhanced stability, toward sustainability and environmental considerations compared to the traditional approaches for extensive potential future use of natural insecticides on large scale (Li et al., 2022; Zhai et al., 2020; Zhong et al., 2017). For example, hexenoic acid, an insect pheromone,

1 was successfully loaded onto zinc layered hydroxide to develop a new generation of
2 environmentally safe pesticide nanomaterial for crop protection (Ahmad et al., 2015). Similarly,
3 some essential oils were loaded onto different clays obtaining an aroma-controlled release systems
4 for pest control (de Oliveira et al., 2022; Saucedo-Zuñiga et al., 2021).

5 Halloysite is a natural clay mineral (JOUSSEIN et al., 2005) derived from weathering rocks present
6 in tropical and subtropical areas since the origin of life. It is an aluminosilicate clay with a
7 predominantly hollow tubular structure with dimensions in the nanometric range and usually, it is
8 referred to as halloysite nanotubes (Hal) (Kogure, 2016; R. Price, 2001). Chemically Hal is similar
9 to the platy kaolinite ($\text{Al}_2\text{Si}_2\text{O}_5(\text{OH})_4 \cdot n\text{H}_2\text{O}$) with an inner surface mainly composed of aluminol
10 groups and an external one constituted by siloxane groups with the presence of few silanols groups
11 as structural defects that are fundamental for chemical modifications of the external surface (Long
12 et al., 2022; Massaro et al., 2018; Massaro et al., 2022a). Generally, the length of the tubes is in the
13 range of 0.2–1.5 μm , while their inner and outer diameters are in the ranges of 10–30 nm and 40–70
14 nm, respectively. The different chemical composition makes the tubes undergo ionization in
15 aqueous media, in a wide range of pH (Bretti et al., 2016). In particular, Hal possesses positive
16 charges in the inner lumen and negative ones at the external surface. The Hal adsorption capacity
17 towards several organic molecules is well documented and the resultant nanomaterials have found
18 applications in several fields (Abdullayev and Lvov, 2011; Massaro et al., 2020; R. Price, 2001).

19 The Hal ability of the controlled release of organic molecules from the lumen is probably the most
20 attractive aspect of this nanomaterial (Ghezzi et al., 2018; Glotov et al., 2021; Hasani et al., 2021;
21 Massaro et al., 2022b; Riela et al., 2021; Santos et al., 2018).

22 Hal is considered a safe material, able to penetrate the cell membranes (Massaro et al., 2022b; Prinz
23 Setter and Segal, 2020), that exerts relevant toxicity in *vitro* at the concentration of 1000 $\mu\text{g/mL}$
24 (Ahmed et al., 2015) whereas in *vivo* the oral administration limit is at ca. 20 mg/kg BW (Long et
25 al., 2018; Wang et al., 2018). Furthermore, it was found that by feeding nematodes with them, no
26 toxic effects were induced (Fakhrullina et al., 2015). The understanding of the phytotoxicity of Hal

1 is helpful for their applications in the environmental protection and agricultural fields (Huang et al.,
2 2021). In this context, some studies were reported about the environmental impact of Hal (Chen et
3 al., 2021a). Recent studies indeed showed that Hal possesses no phytotoxic effects on *Raphanus*
4 *sativus* L (Bellani et al., 2016) and on wheat, while having even positive effect on the growth of
5 tobacco cells and secondary metabolite (Chen et al., 2021b). Furthermore, few studies report the use
6 of Hal as a nanocontainer for pesticides which benefit from sustained and controlled release. Ge et
7 al. for example reported the encapsulation of myrcene into Hal for further environmental
8 applications (Chen et al., 2022; Li et al., 2022). Up to now, for the best of our knowledge, no
9 studies are reported about the delivery of natural pyrethrins by Hal and the subsequent *in vivo*
10 studies on insects as potential pesticides.

11 This study is focused on the advantages that pyrethrins should have if carried by Hal in terms of
12 prevention of photodegradation (da Rocha et al., 2022) (both in solution and in solid state),
13 controlled release (Shao et al., 2022) and toxic effect on model insects.

14 To realize these goals, herein we report the preparation of Hal loaded with pyrethrins from natural
15 pyrethrum extract PESTANALTM (Hal/PE) for domestic or agronomic use. The successful loading
16 of the extract into the Hal lumen was confirmed by thermogravimetric analysis (TGA) and Fourier
17 transform infrared (FT-IR) spectroscopy and the morphology of the nanomaterial was imaged by
18 transmission and scanning electron microscopy measurements (TEM and SEM, respectively). The
19 photostability of the nanomaterial under UV irradiation both in solution and in the solid state was
20 also assessed by UV-vis spectroscopy, circular dichroism, and ESI-MS.

21 Finally, as proof of concept, the toxic effects of the Hal/PE obtained, were evaluated *in vivo* on
22 selected target insects, i.e., adults of the yellow mealworm *Tenebrio molitor* L. and young larvae of
23 the greater wax moth *Galleria mellonella* (L.) in terms of mortality and sub-lethal effects induced in
24 the target insects. The two insects are respectively known as pests of stored grains and foodstuff
25 (Hill, 1990) and of *Apis mellifera* L. hives (Kwadha et al., 2017), respectively. Moreover, *G.*
26 *mellonella* larvae are widely used as model insects in laboratory trials, since they may be

1 maintained quite easily in continuous colonies, with relatively low production costs, they show a
2 quite rapid life cycle (about 6 weeks), survival at 30°C - 35°C, and generally do not require ethical
3 permits (Dindo et al., 2003; Ignasiak and Maxwell, 2017; Kay et al., 2019). The results support the
4 potential use of nanomaterials based on Hal and pyrethrins as natural pesticides, as well as the
5 safety nature of the resulting organic/inorganic nanomaterial ensures new environmentally friendly
6 pesticides.

7 **2. Materials and Methods**

8 The pyrethrum extract (PE), PESTANALTM (extract botanical insecticide, CAS 8003-34-7 -
9 analytical standard), was purchased from Sigma-Aldrich Chemical Co, and used without further
10 purification. Depending on the batch used it contains 40.7 wt% (Batch number: BCBZ5050) or ca.
11 54 wt% (Batch number: BCCD5535), of pyrethrins content. In particular, the first batch was used
12 for the photodegradation studies, and the second one for the preparation and characterization of
13 Hal/PE nanomaterial. Halloysite (Merck) was used as purchased without further purification. It
14 presented an average tube diameter of 50 nm and an inner lumen diameter of 15 nm. Typical
15 specific surface area is 65 m² g⁻¹; pore volume of ~1.25 cm³ g⁻¹; refractive index 1.54 and specific
16 gravity 2.53 g cm⁻³.

17 Commercial pyrethrum used as a positive control in *in vivo* studies was from Bayer (Pyrethrum
18 Actigreen).

19 FT-IR spectra (KBr) were recorded with an Agilent Technologies Cary 630 FT-IR spectrometer.
20 Specimens for these measurements were prepared by mixing 5 mg of the sample powder with 100
21 mg of KBr.

22 GC-MS used was on a single quadrupole Shimadzu GC-MS-QP2010 Plus equipped with an AOC-
23 20i autoinjector (Shimadzu, Kyoto, Japan) and a Supelcowax 10 capillary column (30 m long, 0.25
24 mm i.d., 0.25 µm film thickness). One µl of each sample was injected at 250°C in the splitless
25 mode, and the column flow (carrier gas: helium) was set at 1 mL/min. The GC oven temperature
26 was held for 5 min at 40°C, then increased by 2°C/min to 250°C, held for 15 min, and finally raised

1 to 270°C at 10°C/min. The MS interface worked at 280°C, and the ion source at 250°C. Mass
2 spectra were taken at 70 eV (in EI mode) from m/z 30 to 500. The GC/MS data were analysed using
3 the GCMSolution package, Version 2.7.

4 For Transmission Electron Microscope (TEM) observation the samples were prepared using a drop
5 of water suspension on a formvar coated copper grid (400 mesh) and allowing the drop to dry
6 completely in a vacuum desiccator. The TEM images of the samples were obtained using a Philips
7 TEM CM 100 transmission electron microscope at accelerating voltage = 80 kV.

8 The thermogravimetric analysis (TGA) of the material was performed in a TGA/DSC1 STAR
9 System from Mettler Toledo Inc. The sample (15 mg) was subjected to a pre-treatment in air flow
10 (30 mL/min) from 25°C to 100°C with a heating rate of 10°C/min and holding time at 100°C for 30
11 min, to remove any eventual physisorbed water. Then, the temperature was increased from 100 to
12 1000°C under air flow (30 mL/min) and the weight loss occurring during this step was considered
13 to calculate the organic weight content of the Hal/PE nanomaterial.

14 The various components of the aqueous pyrethrum extract were analysed by a UPLC
15 chromatographic system, Waters ACQUITY H-CLASS model, coupled with a Waters Xevo G2-XS
16 QToF (Waters) mass spectrometer, with an ESI-APCI type source. UPLC conditions: ramp rate
17 accelerated to 2 mL/min in 0.45 min, mobile phase A was water, B was acetonitrile.

18 Xevo G2-XS QToF conditions: Positive mode, Cone Voltage: 20 V, Capillary: 0.8 kV, Collision
19 Energy: 6.00 eV, Source Temperature: 120°C, Desolvation Temperature: 600°C, Cone Gas Flow:
20 50 L/h, Desolvation Gas Flow: 1000 L/h.

21 UV-vis spectra were acquired on a Jasco V-550 spectrophotometer.

22 Circular Dichroism (CD)/UV measurements were performed at room temperature on a Jasco J-715
23 spectropolarimeter. Spectra were recorded at a scanning speed of 100 nm/min and five consecutive
24 scans in the 400-205 nm range were averaged for each sample. Electrospray ionization mass
25 spectrometry (ESI-MS) analysis was carried out on a Micromass ZQ-4000 single quadrupole mass
26 spectrometer operating at 4000 m/z. An infusion syringe pump was used for direct injection of the

1 sample at a rate of 10 μ l/min. Operating parameters were: capillary voltage 3 kV, cone voltage 30
2 V, capillary temperature 120°C, desolvation temperature 220°C. Mass analysis was carried on in
3 the 100-1300 amu range (positive ionization mode).

4 **2.1 Synthesis of the Hal/PE nanomaterial**

5 To a dispersion of Hal (100 mg) in water (5 mL), pyrethrum extract (50 mg) was added. The
6 suspension was sonicated for 5 min, at an ultrasound power of 200 W and at 25°C, and was left
7 under stirring for 18 h at room temperature. After this time, the dispersion was centrifuged and the
8 obtained powder was washed with water, until the unreacted pyrethrins were removed and, then
9 dried at r.t. The loading and loading efficiencies (LD% and LE%, respectively) were calculated as
10 follows by using Eq. 1 and 2.

11 Ca. 2 mg of Hal/PE nanomaterial were carefully weighed and washed with four portions of hexane
12 (2 mL each). The organic solution obtained was then analyzed by GC-MS.

$$13 \quad LD\% = \frac{m_{\text{pyrethrins_Hal}}}{m_{\text{Hal}} + m_{\text{pyrethrins_Hal}}} \times 100 \quad (\text{Eq. 1})$$

$$14 \quad LE\% = \frac{m_{\text{pyrethrins_Hal}}}{m_{\text{pyrethrins_TOT}}} \times 100 \quad (\text{Eq. 2})$$

15 where $m_{\text{pyrethrins_Hal}}$ and $m_{\text{pyrethrins_TOT}}$ are the amount (express in mg) of the pyrethrins loaded on Hal
16 and the total feed one, respectively and m_{Hal} is the mass of Hal (express in mg).

17 **2.2 Photodegradation studies in solution**

18 Different aliquots of an aqueous suspension of PESTANALTM (0.03 mg/mL) or aqueous dispersion
19 of Hal/PE (0.25 mg/mL) were placed under UV lamp (254 nm, 32 W, with a distance of 15 cm, at
20 room temperature). The sample into a closed UV quartz cuvette (total volume 2 mL) was exposed
21 to the lamp. For PESTANALTM, after predetermined times, the aqueous solutions were analysed
22 and the percentage of decomposed pyrethrins was determined by spectrophotometric measurements
23 estimating the disappearance of the maximum absorption band of pyrethrum (226 nm) and by
24 UPLC-ESI-MS.

1 In the case of Hal/PE dispersions, 2 samples were irradiated at 254 nm for 1 h and 4 h respectively.
2 After the set time, both samples were stirred vigorously for four minutes with 2 mL of hexane, to
3 extract residual pyrethrins. UV spectra were recorded on the obtained hexane solutions. A
4 comparison with a non-irradiated sample was carried out. All experiments were carried out in
5 duplicate at 25°C.

6 **2.3 Photodegradation studies in solid state**

7 Irradiation experiments were performed by using a UV-*vis* medium-pressure Mercury 125 W lamp.
8 Each sample was inserted into a rectangular UV quartz cuvette (1 × 1 cm, total volume 3 mL) by
9 accurate deposition over a selected wall of the cell. In particular, 2.9 mg of Hal/PE nanomaterial
10 were uniformly distributed, while a thin film of PESTANALTM was prepared upon deposition of 4
11 × 25 µL of a 3 mg/mL hexane solution quickly drying at room temperature. Each cuvette,
12 appropriately closed, was placed with the selected wall exposed to the lamp at a distance of 7 cm
13 and inclined by 45°. The temperature of samples during irradiation did not exceed 22°C. After the
14 desired irradiation time the PESTANALTM film was dissolved in 6.5 mL of hexane, while the
15 Hal/PE nanomaterial was dispersed in 6.5 mL of hexane and vigorously stirred for 30 minutes for
16 pyrethrin extraction: the supernatant was recovered upon ultracentrifugation at 5000 rpm for 10
17 min. All the obtained hexane solutions were preliminarily analyzed by CD/UV spectroscopy by
18 using a 1 cm quartz cell. For ESI MS analysis a good correlating calibration curve was obtained in
19 methanol for PESTANALTM concentrations ranging from 0.189 to 0.027 mg/mL and by using
20 glucose 0.14 mM as an internal standard. Thus, for ESI MS analysis all hexane samples were dried
21 under nitrogen and dissolved in the appropriate amount of methanol in the presence of glucose 0.14
22 mM. For each experiment, two replications were carried out

23 **2.4 Kinetic Release**

24 The release of pyrethrins from Hal/PE nanomaterial was performed as follows: 9.5 mg of the
25 sample were transferred into a dialysis membrane (Medicell International Ltd MWCO 12–14,000
26 with a diameter of 21.5 mm) and wet with 0.5 mL of water. The membrane was then put in a round

bottom flask containing 4.5 mL of water at 25°C under constant stirring. At fixed times, 0.5 mL of the release medium was withdrawn and analyzed. To keep constant the volume of the release medium 0.5 mL of water was added each time to replace the withdrawn one. Each sample was extracted three times with 0.5 mL of hexane, dried under nitrogen and dissolved in 0.5 mL of hexane. The pyrethrins concentration in the solution was determined by UV-vis spectrophotometry using the Lambert-Beer law, measuring the absorbance at 224 nm, by assuming that at each time all pyrethrum components were proportionally released.

Total amount of pyrethrins released (F_t) was calculated as follows:

$$F_t = V_m C_t + \sum_{i=0}^{t-1} V_a C_i \quad (\text{Eq. 3})$$

where V_m and C_t are the volume and concentration of pyrethrum at time t . V_a is the volume of the sample and C_i is pyrethrins concentration at time i ($i < t$).

2.6 Activity Hal/PE on insects

2.6.1 Insects

T. molitor specimens were kept in plastic boxes (30 × 18 × 10 cm) at 25 ± 1°C, 65 ± 5% R.H. and L16:D8 photoperiod. Food consisted of cracker pieces, corn flour, and carrots as a source of hydration. To obtain adults of similar age, *T. molitor* pupae were transferred from the colony to a separate box provided with food. After about one week, the newly emerged adults were collected and used in trials.

G. mellonella larvae were reared in plastic boxes (24 × 12 × 8 cm) at 30 ± 1°C, 65 ± 5% R.H. and L0:D24 photoperiod and fed on an artificial diet (Dindo et al., 2003; Marchetti et al., 2009). Young larvae (in the 3rd or 4th instar, approximately 1-1.5 cm long) were used in the trials.

Laboratory colonies of *T. molitor* and *G. mellonella* were maintained at the Department of Agricultural and Food Sciences of University of Bologna.

2.6.2 Toxic effects of Hal/PESTANAL™ vs. PESTANAL™ and commercial pyrethrum extract

1 The efficacy of Hal/PE nanomaterial (1 mg/mL corresponding to 0.02 mg/mL in pyrethrins) and
2 commercial pesticides (Pyrethrum Actigreen 0.04 mg/mL, PESTANALTM 0.04 mg/mL) was tested
3 by contact bioassays, separately for *T. molitor* and *G. mellonella*. Distilled water was maintained as
4 control.

5 In each treatment 1 mL liquid product was pipetted onto the bottom of a 6 cm diameter plastic petri
6 dish. Insects (either *T. molitor* adults or *G. mellonella* larvae) were then placed in the dish which
7 was eventually covered with its lid.

8 For each insect species, 6 replicates per treatment were set up, each consisting of one petri dish with
9 5 individuals, with 90 insects in total per species (30 per treatment). All petri dishes were
10 maintained in an incubator at $25 \pm 1^\circ\text{C}$, $65 \pm 5\%$ R.H., and L16:D8 photoperiod.

11 In all treatments, the number of dead individuals was counted at three check times, i.e., 24 h, 72 h,
12 and 168 h (1 week) post insect exposure. Sub-lethal effects (i.e., the number of individuals showing
13 low mobility) were also detected at each check time.

14 *Parameters*

15 In both trials, for each insect species and at each check time, mortality (%) was calculated over the
16 original insect number ($n = 5$ per replicate per treatment). At each check time, the number of
17 survived healthy individuals and of low mobile individuals was also calculated. For each treatment,
18 these data were pooled for all replicates.

19 *Statistical analysis*

20 Percent mortalities were analyzed by one-way ANOVA or by Kruskal-Wallis test, respectively
21 followed by Tukey's HSD test or non- parametric multi-comparisons when a significant difference
22 occurred. The Kruskal-Wallis test was used in case of variance heterogeneity (p-value > 0.05,
23 Levene test). Prior to analysis, the percentage values were angular transformed by means of
24 Freeman-Tukey double arcsine transformation for small samples ($n < 50$) (MOSTELLER and
25 YOUTZ, 1961). To compare low mobile vs. healthy alive individuals, 2×2 contingency tables

were created, using Yates correction for small numbers (<100). Data analysis was performed with the statistical program STATISTICA v.10.0 (StatSoft, Tulsa, OK, USA).

3. Results and Discussion

Pyrethrum extract is a mixture of different components, where the main ones are the so-called pyrethrins (Pyrethrin I, Pyrethrin II, Cinerin I, Cinerin II, Jasmolin I, and Jasmolin II). Based on the physico-chemical properties of both Hal and PE components, the interaction between them can occur by electrostatic attraction interactions, hydrophobic effects, and hydrogen bonding occurring between the Al-OH groups present at the inner surface of Hal and the oxygen atoms of the PE components (Figure 1).

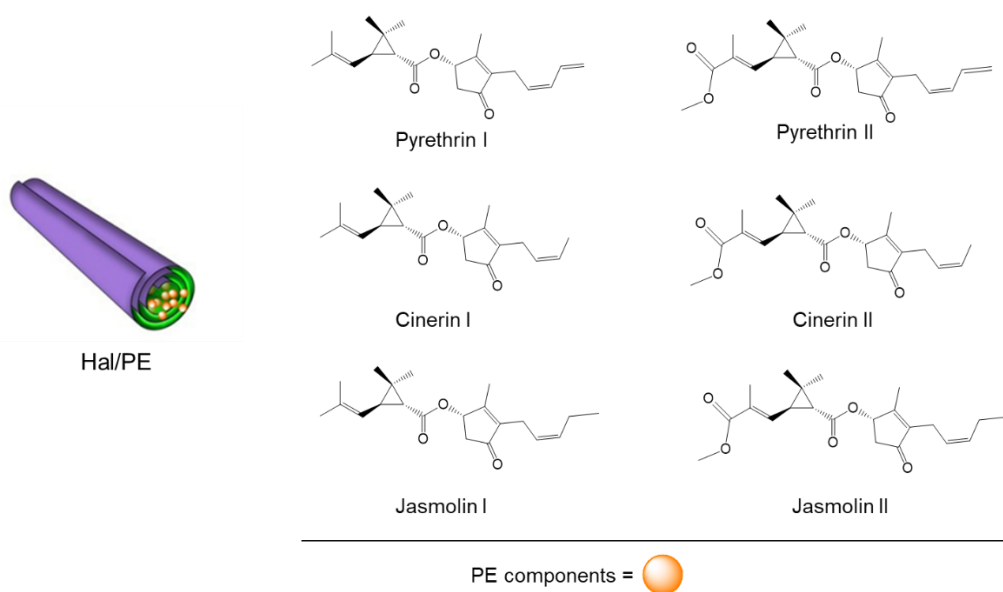


Figure 1. Schematic representation of the Hal/PE nanomaterial synthesized.

The main components of pyrethrum extract from PESTANALTM (PE) were loaded into Hal by adopting a procedure reported elsewhere (Massaro et al., 2022b; Riela et al., 2021). After the work-up the amount of extract loaded on Hal, was estimated by GC-MS analysis and was found to be ca. 5.5 wt% with an entrapment efficiency of ca. 30%.

Noteworthy, the GC-MS analysis highlighted that the main components of pyrethrum extract are loaded onto Hal in the same molar ratios as present in the extract itself (Figure 2).

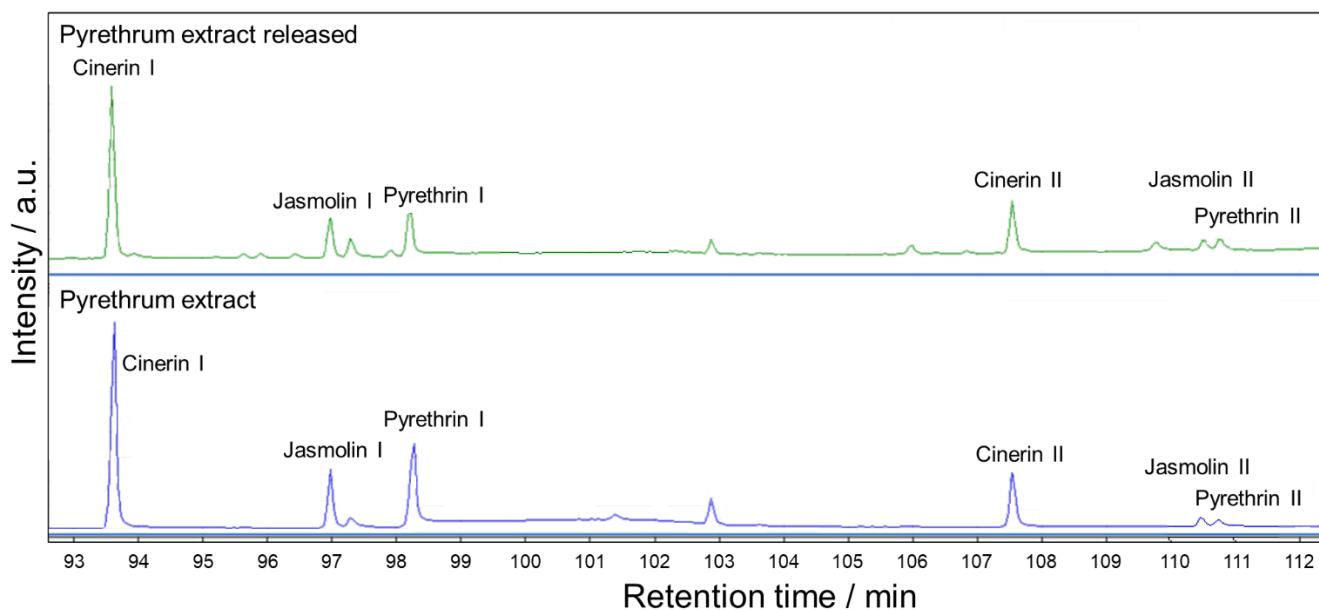


Figure 2. GC-MS analysis of the commercial pyrethrum extract (PESTANALTM) and the pyrethrum extracted from Hal/PE nanomaterial.

The successful loading was verified by FT-IR spectroscopy and thermogravimetric analysis. The FT-IR spectrum of the Hal/PE nanomaterial shows the typical vibration bands of HNTs, namely the bands at 3622 and 3493 cm^{-1} corresponding to O–H stretching vibrations of buried hydroxyl groups and inner surface hydroxyl groups, respectively, and the bands at 3484 and 1645 cm^{-1} assigned to O–H stretching vibrations of adsorbed water. Besides these, some additional bands, related to the PE, are present corroborating the loading of pyrethrum components (Pajnik et al., 2018) (Figure 3a). In particular, the bands related to the C–H asymmetric and symmetric stretching vibrations of pyrethrins at ca. 2900 and 2850 cm^{-1} are clearly observable together with the band at ca. 1715 cm^{-1} ascribed to the stretching of C=O group, and the band at ca. 1500 cm^{-1} attributable to the stretching of C=C group of pyrethrins skeleton. Finally, the band at ca. 1200 cm^{-1} was due to the stretching vibration of C–O groups.

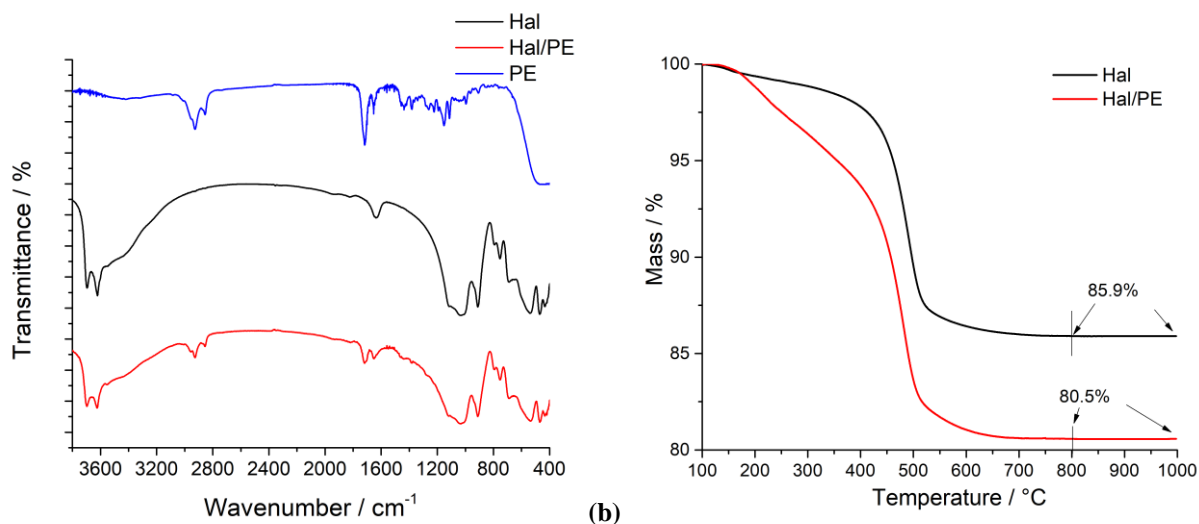


Figure 3. (a) FT-IR spectra pristine Hal, PE, and Hal/PE nanomaterial and (b) TGA curves of pristine Hal and Hal/PE nanomaterial.

Pristine pyrethrum extract totally decomposes in a multi-step process occurring in a temperature range between 200 and 450°C (Figure S1). As results from the comparison of the TGA curves (Figure 3b) the pristine Hal and Hal/PE nanomaterial show different thermal stability under air atmosphere by increasing the temperature from 100°C up to ca 600°C. In both cases, a negligible weight loss occurs between rt up to 100°C due to removal of some physically adsorbed water (this step was omitted in the shown figure) The Hal exhibits relatively good stability up to ca 350°C, then between 350 and 600°C, suddenly lose weight until reaching a stable value corresponding to ca 86 wt% of the initial mass.

Accordingly, with the literature (Massaro et al., 2020) a progressive dehydroxylation of the structural Al-OH groups of the Hal occurs until complete structural modification, at around 550-600°C. The Hal/PE nanomaterial according to the presence of pyrethrum, an organic ester, starts to be degraded earlier than the pristine Hal, starting from~ 200°C, losing weight increasingly by increasing the temperature up to 600°C, up to stable mass corresponding to 80.5 wt%.

The amount of PE loaded into Hal was calculated by using the rule of the mixture by considering the mass losses at 25–150°C (ML₁₅₀) and the residual masses at 800°C (MR₈₀₀) for the pristine components (Hal and PE) and the Hal/PE nanomaterial (Lisuzzo et al., 2020; Lisuzzo et al., 2019).

1 In Table 1 the ML_{150} and MR_{800} values of PE, Hal and Hal/PE nanomaterial are reported. From
 2 these data it was possible to calculate the loading efficiency that was of ca. 5.5 wt% in agreement
 3 with GC-MS analysis.

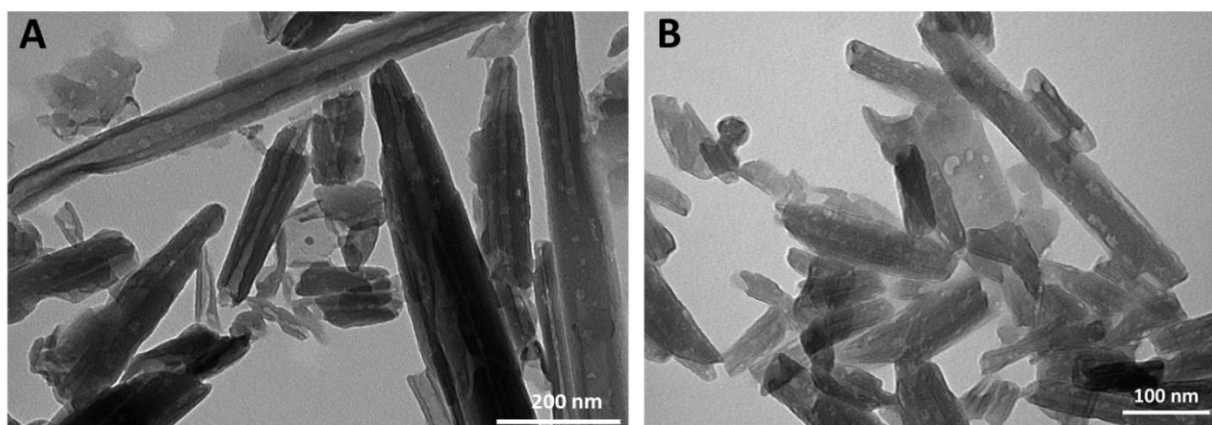
4 Details on the calculation of the loading amounts of PE into Hal are shown in SI.

5 **Table 1.** Thermogravimetric parameters for PE, Hal and Hal/PE nanomaterial.

	ML_{150} / wt%	MR_{800} / wt%	MD_{800} / wt% ^a
PE	0	0	100
Hal	3.0	85.9	11.2
Hal/PE	3.0	80.5	16.5

6 ^a for the calculation of MD_{800} (degraded matter) values see SI.

7 The morphology of the Hal/PE nanomaterial was imaged by TEM and SEM measurements. As it is
 8 possible to note, after the extract loading the tubular morphology of Hal is preserved (Figure 4A).
 9 However, TEM image shows that the Hal lumen is not apparent in all its length confirming the
 10 successful loading (Figure 4B). Furthermore, the EDX analysis showed that beside the presence of
 11 the Al, Si and O atoms related to the inorganic carrier, C atoms are present in the nanomaterial,
 12 further confirming the loading (Figure 4C).



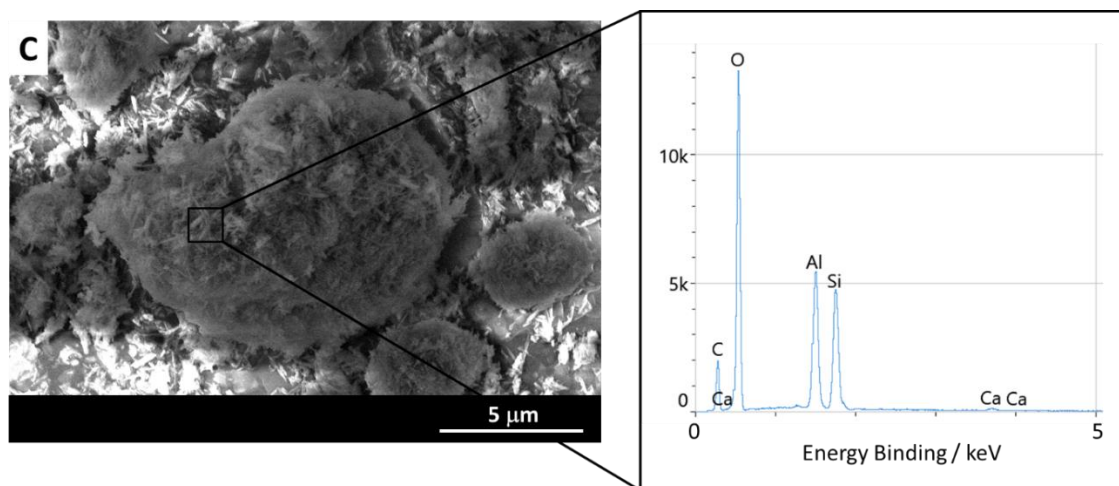


Figure 4. (A-B) TEM images of (A) raw Hal and (B) Hal/PE nanomaterial, (C) SEM image of Hal/PE nanomaterial, the insert shows the EDX analysis on the selected area.

3.3 Kinetic release

To evaluate the performances of the Hal/PE nanomaterial for potential application as a pesticide, the kinetic release of the pyrethrins, constituents of PE extract, from Hal/PE nanomaterial was evaluated by the dialysis bag method, using the same conditions adopted for the *in vivo* experiments (water, 25°C) and the obtained kinetic data are shown in Figure 5. In the same conditions, the PE spreading through the membrane is hampered by its very low solubility in water.

As it is possible to notice from Figure 5, a slow release occurred in the first 300 minutes after which a plateau is observed. Indeed, only 14 wt% of the total amount of pyrethrins loaded into Hal was released after 48 h indicating that the Hal could act as a reservoir for a slow release of pesticides.

To better understand the release mechanism, the kinetic data were analyzed by the first order and power fit models. The mathematical analysis showed that the kinetic data are better fitted by the first order model ($M_{\infty} = 9.7 \pm 0.3$ mg/mL, $k = 0.014 \pm 0.001$ min⁻¹, $R^2 = 0.9887$), indicating a simple diffusion of the pyrethrins from Hal lumen.

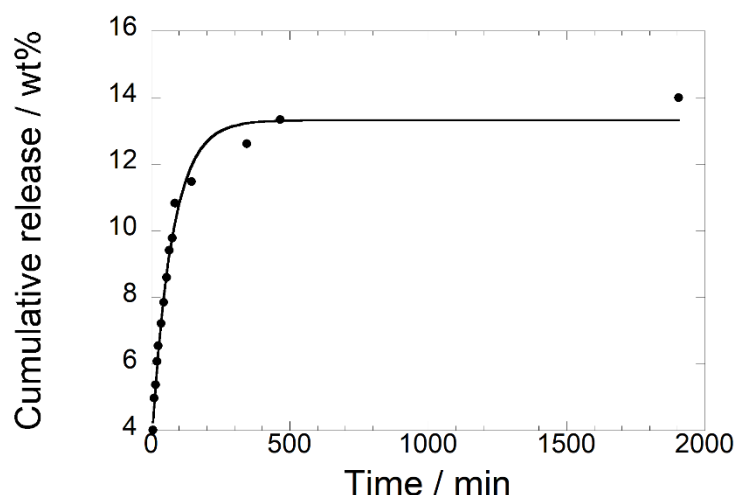


Figure 5. Kinetic release of pyrethrins from Hal/PE nanomaterial at 25°C in water.

3.4 Photodegradation studies

In the last years, pyrethrins were largely replaced by their synthetic derivatives, pyrethroids. However, due to their harmful effects on various species, the use of pyrethrins should again take the lead. Pyrethrins indeed possess, among other interesting properties, less negative effects on the environment compared to synthetic ones (Chrustek et al., 2018).

One of the major drawbacks of the agricultural use of pyrethrum extract is its rapid photodegradation under UV light. Therefore, the assessment of the photostability of the obtained nanomaterial in solution and in solid state is relevant for its possible future use as a pesticide indoors and outdoors. In this section, we report on the photostability of the Hal/PE nanomaterial in comparison with the pyrethrum extract both in solution and in a solid state.

3.4.1 Photostability in solution

Inspired by recent photochemical studies performed on pyrethrin formulations (Zhang et al., 2019), we firstly tested the photostability of PESTANALTM and Hal/PE nanomaterial in water under UV irradiation at 254 nm. The amount of pyrethrins photodegraded as a function of time was determined by UV-vis measurements. As far as is regarding the pyrethrum extract, pyrethrin degradation followed a pseudo-first-order model ($R^2 = 0.994$), the process in aqueous solution was

1 very rapid ($k_{obs} = 0.07 \text{ min}^{-1}$), with a degradation rate higher than 50% after about 10 min (Figure
2 S2).

3 The decay of each component of the PESTANALTM was also assessed by UPLC-ESI-MS. As found
4 by UV-*vis* measurements, pyrethrins were almost totally photodegraded within 20 min of irradiation
5 (Figure 6).

6 Noteworthy, conversely to experimental results obtained for the PESTANALTM, after the pyrethrins
7 loading into Hal, no photodegradation occurred in the first 60 min. Indeed, UV spectra obtained by
8 a Hal/PE water dispersion before and after irradiation (Figure S3) show that signal intensity, related
9 to pyrethrin content, reduced less than 10% after 60 min and about 15% after 4 h, presumably due
10 to molecular release in water and consequent photodegradation. On the other hand, almost 90% of
11 initial pyrethrins were found active after 60 min, as presumably still included in Hal/PE and then
12 photoprotected. This result agrees with the very slow release of pyrethrins from Hal/PE
13 nanomaterial in aqueous medium described above, and in parallel highlights the shielding ability of
14 halloysite against the short-wavelength UV radiations (UV-C range). Similar results were found by
15 Liu et al. which demonstrated that the UV reflection by the Hal layered silicate structures greatly
16 improved the effective UV protection time of the pesticide chlorpyrifos (Qin et al., 2022).

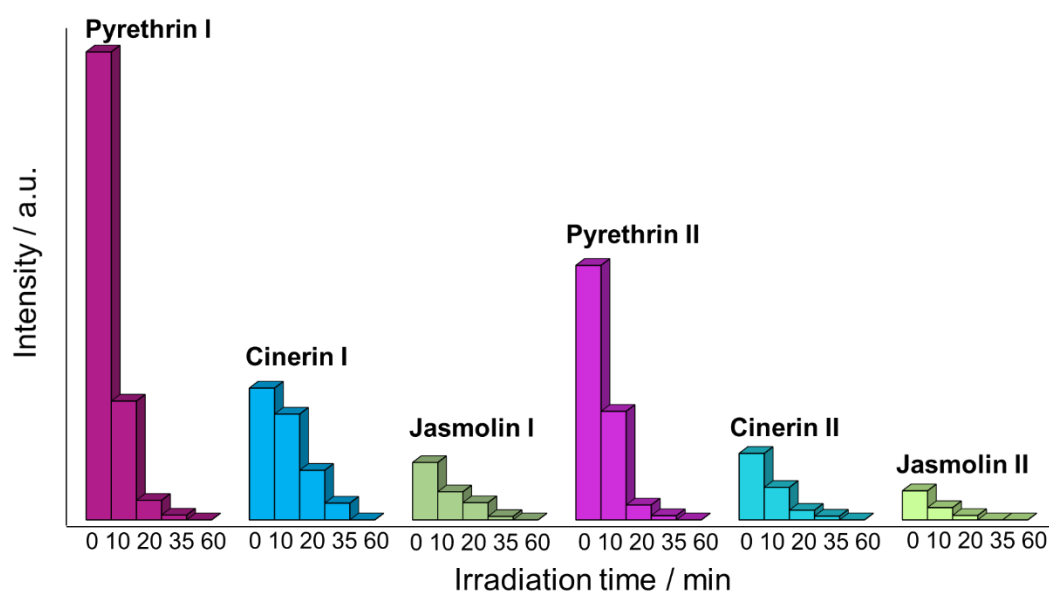


Figure 6. Photodegradation of PE components (Pyrethrin I and II, Cinerin I and II, Jasmolin I and II) in water as a function of time.

3.4.2 Photostability in solid state

A deeper investigation on photostability of Hal/PE was performed on the solid state. In this case a mercury lamp, that includes UV-B and UV-A emissions, was used for irradiation experiments to better mimic natural UV light. The Hal/PE nanomaterial and a PESTANALTM film, used as control, were subjected to UV light irradiation, and consequent photodegradation was monitored by UV/CD spectroscopy and ESI-MS. In accordance with pyrethrin maximum absorbance (Head, 1973) UV spectra exhibited a maximum at *ca.* 225 nm (Figure 7) and due to the chirality of the six components - related to their insecticidal activity (Kawamoto et al., 2020), the same spectral region was dominated by a negative CD band. A positive CD signal was also detected between 300 and 350 nm (Figure S4) (Crombie, 1999). Upon UV irradiation of PESTANALTM a gradual lowering of either UV or CD signals diagnostic of progressive PE components photodecomposition was observed. In particular, after two hours UV/CD absorption maxima were reduced to *ca.* 30%. Conversely, in the case of Hal/PE nanomaterial more than 60% of both UV and CD signal intensities were preserved after 4 hours of irradiation (Figures 7 and S4). These preliminary results suggested that PE lifetime under ultraviolet light exposition was significantly enhanced by loading into Hal.

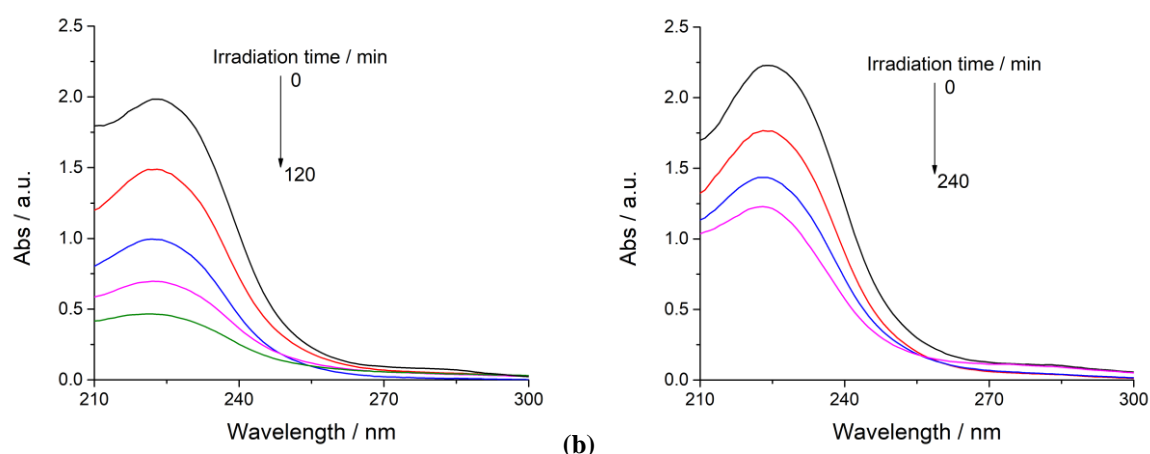


Figure 7. UV spectra recorded on solutions obtained by treating with a volume of hexane (a) the PESTANALTM film and (b) the Hal/PE nanomaterial after different irradiation times with ultraviolet light.

UV/CD data were corroborated by ESI MS analysis that provided identification and quantification of the individual components (Figures S5 and S6). The obtained plots showing the percentage of remaining pyrethrins vs the irradiation time are depicted in Figure 8. For the PESTANALTM sample, the initial pyrethrin content reduced to 47% after one hour and to 35% after two hours. Conversely, after 2 h irradiation of the Hal/PE nanomaterial, ca. 61% of the total amount of PE into the lumen was recovered and noteworthy, more than 50% of the initial amount was still present after four hours, as testified by the analysis of hexane solution of the PE extracted from Hal/PE nanomaterial (Figure 8). Collected data highlighted for the Hal/PE nanomaterial a significant improved photostability in respect to PESTANALTM. Weakening of UV radiation interacting with the Hal walls accompanied by possible absorption of the lowest wavelengths shall be responsible for the observed protective effect (Cavallaro et al., 2020).

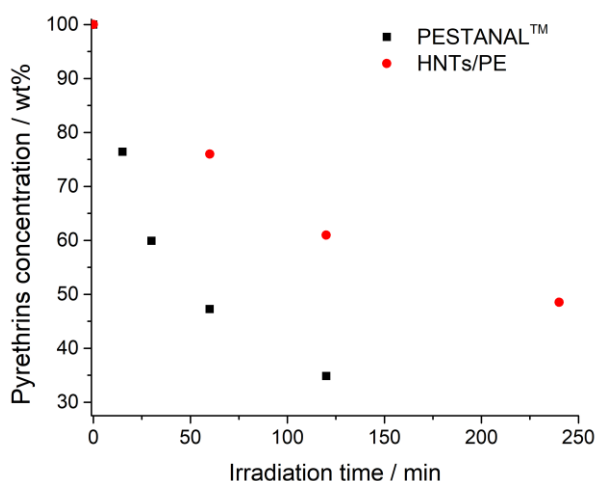


Figure 8. Percentage of remaining pyrethrins (wt%) after different UV irradiation times of the Hal/PE nanomaterial and the PESTANALTM film.

3.5 Toxic activity of Hal/PE nanomaterial vs *T. molitor* and *G. mellonella*.

It is known that pyrethrins pass through the exoskeleton of insect chitin by contact diffusion and cause depolarization by preventing the closure of the sodium channels of the cell membrane in nerve and muscle cells (Kaya, 2020).

As proof of concept, the toxic effects of the developed Hal/PE nanomaterial were tested *in vivo* on selected target insects, i.e., adults of the yellow mealworm *T. molitor* and young larvae of the greater wax moth *G. mellonella* in terms of mortality and sub-lethal effects induced in the target

1 insects. Hal did not show any toxic effects on the target insects in the experimental conditions used.

2 Firstly, the Hal/PE nanomaterial and commercial pesticides were used at the concentration

3 recommended for field application (2 mg/mL, corresponding to 0.04 mg/mL of PE components and

4 0.04 mg/mL for Hal/PE nanomaterial and commercial pyrethrins, respectively). In these conditions,

5 no differences between the two treatments were observed. Therefore, we tested the Hal/PE

6 nanomaterial at a concentration of 1 mg/mL, corresponding to 0.02 mg/mL of PE components.

7 Table 2 reports the results obtained in terms of mortality of the two insects after different exposure

8 times to the Hal/PE nanomaterial and PESTANALTM (similar results were obtained in the case of

9 the Pyrethrum Actigreen[®]).

10 As it is possible to observe, after 24 h of exposure, the mortality of *G. melonella* was ca. 97-100%

11 for both Hal/PE nanomaterial and commercial pesticide. At each check time, mortality in the

12 negative control (distilled water) was extremely low (Table 2). This result was noteworthy, since

13 the presence of Hal allowed to halve the amount of pyrethrins used without differences in the

14 pesticide activity, in comparison to the concentration commonly recommended for this kind of

15 treatments. This finding could be a consequence of the presence of Hal which both protect the

16 pyrethrins molecules from photodegradation and hydrolysis and at the same time, it enhances their

17 aqueous solubility improving the pesticide activity.

18 Regarding the yellow mealworm adults, the results were quite different. In this case, indeed, no

19 significant mortality of the insects was observed in the first 48 h of all treatments. After 1 week of

20 exposure, eventually, ca. 35% of mealworms were found dead without any appreciable difference in

21 each case investigated. These results could be explained by considering the different characteristics

22 of the two insects. Natural pyrethrins, like their synthetic derivatives pyrethroids, do not act as a

23 repellent towards insects, but, rather, as contact insecticide, causing nervous system toxicity,

24 leading to death or “knockdown” of the insect. Therefore, their action on *T. molitor* adults, which

25 are hard-shelled beetle, could be limited by their scarce uptake.

26

1 **Table 2.** Mortality (%) of *T. molitor* adults and *G. mellonella* larvae observed in the first trial. Individuals were
2 treated by contact with Hal/PE nanomaterial (1 mg/mL, corresponding to a pyrethrin concentration of 0.02
3 mg/mL), commercial pesticides (0.04 mg/mL) or negative control (water). Mean values (\pm SE) at each check time
4 (24 h, 72 h, and 1 week post insect exposure) are reported. Number of replicates = 6. At each time, % mortality
5 was calculated on the original number of individuals (5 per treatment per replicate= 90 individuals per insect
6 species). Means in a column followed by the same letter are not significantly different ($P < 0.05$) by one-way
7 analysis of variance followed by Tukey's HSD test (yellow mealworms - 72 h) or Kruskal-Wallis test followed
8 by non-parametric multi-comparisons (other parameters).

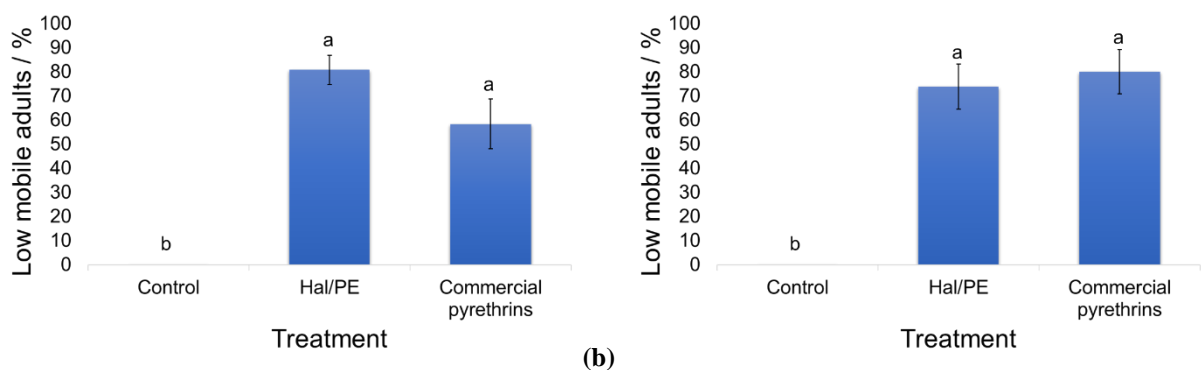
<i>G. mellonella</i>			
Treatment	Mortality (%) (24 h)	Mortality (%) (72 h)	Mortality (%) (1 week)
Hal/PE	100 a	100 a	100 a
Commercial Pesticides*	97 \pm 3 a	100 a	100 a
Distilled water	0 b	0 b	3 \pm 3 b
H (N)	15.6 (18)	17 (18)	16.6 (18)
P	0.0004	0.0002	0.0002

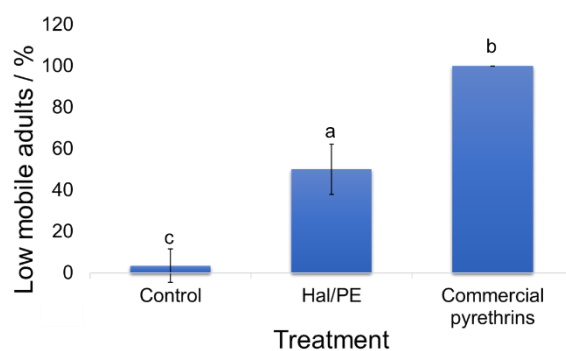
9

<i>T. molitor</i>			
Treatment	Mortality (%) (24 h)	Mortality (%) (72 h)	Mortality (%) (1 week)
Hal/PE	13 \pm 10 a	23 \pm 16 a	29 \pm 10 a
Commercial Pesticides ^a	17 \pm 10 a	33 \pm 13 a	36 \pm 9 a
Distilled water	0 a	3 \pm 3 a	15 \pm 3 b
F (df)		1.7 (2.15)	
H (N)	3.5 (18)		7.0 (18)
P	0.175	0.208	0.03

1 *PESTANAL™ or Pyrethrum Actigreen®.

2 However, by checking the mobility of the survived individuals at each exposure time investigated, it
3 was found that the treatment with both Hal/PE and PESTANAL™ resulted in significantly lower
4 mobility of survived individuals, in comparison to the negative control (24 h: $\chi^2 = 35.40$, $df = 1$, P
5 < 0.0001 for Hal/PE nanomaterial; $\chi^2 = 20.69$, $df = 1$, $P < 0.0001$ for PESTANAL™; 72 h: $\chi^2 =$
6 28.58 , $df = 1$, $P < 0.0001$ for Hal/PE nanomaterial; $\chi^2 = 30.91$, $df = 1$, $P < 0.0001$ for
7 PESTANAL™; 168: $\chi^2 = 11.72$, $df = 1$, $P = 0.0006$ for Hal/PE nanomaterial; $\chi^2 = 37.99$, $df = 1$, P
8 < 0.0001 for PESTANAL™) (Figure 9). No significant difference was found between the two
9 treatments both at 24 h ($\chi^2 = 2.02$, $df = 1$, $P = 0.1554$) and 72 h ($\chi^2 = 0.01$, $df = 1$, $P = 0.9129$) after
10 exposure. Surprisingly, after one week of treatment with the Hal/ PE nanomaterial the number of
11 low mobile adults was lower than at 72 h (Figure 9b and 9c). This result suggests that the survived,
12 low mobile, yellow mealworm adults overtime showed some capacity to retrieve. Since it is known
13 that low dosages of pyrethrins led to a recovery of the insects from the exposure (Soderlund, 2010),
14 the experimental results are in agreement with the slow release of PE components from Hal/PE
15 nanomaterial. After 1 week treatment with PESTANAL™, indeed, the number of low mobile adults
16 (100%) was significantly higher compared with Hal/PE nanomaterial ($\chi^2 = 8.97$, $df = 1$, $P = 0.0027$)
17 (Figure 9c).





(c)

Figure 9. Sub-lethal effects of Hal/PE nanomaterial and PESTANALTM on *T. molitor* adults in contact bioassays. Columns indicate the percentage (\pm SE) of low mobile adults, calculated over the total number of alive adults, at three check times: (a) 24 h, (b) 72 h and (c) 1 week after placing the insects in the treated petri dishes. In each graph, different letters above the columns indicate significant differences in the percentage of low mobile adults as determined by 2×2 contingency tables, created to test any possible combination of treatments. At each check time, the numbers of alive adults for Hal/PE nanomaterial, PESTANALTM and water were 26, 24 and 30 (24 h); 23, 20 and 29 (72 h) and 18, 17 and 29 (1 week), respectively.

4. Conclusions

In summary, a novel system for the controlled release and UV protection of pyrethrum extract components was obtained using Hal as nanocontainer. The combination of the eco-friendly clay mineral and pyrethrum improves the photochemical stability of the extract, both in solution and in the solid state, enhances its water solubility, and pesticidal activity in the *in vivo* models considered. Hal offers some advantages over other nanomaterials already reported for these purposes (Wibowo et al., 2014; Yan et al., 2019), because of its low-cost, large, and natural availability and its intrinsic properties such as photoprotective effects. Similarly to other clay minerals (da Rocha et al., 2019), indeed, Hal chemical and structural features render it a good photoprotective material for different organic molecules. Specifically, in this study, it was demonstrated that the encapsulation of pyrethrum extract components into Hal lumen, prevents their photodegradation. Irradiation of Hal/PE nanomaterial both in solution and in the solid state showed that the clay protected the PE

1 from UV light for at least 4 h, conversely, the pristine PE was fully photodegraded after 1 h of
2 irradiation.

3 *In vivo* tests performed on *G. mellonella* and *T. molitor* showed that the pyrethrins loaded onto Hal
4 possess the same activity as standard pyrethrins, at half dose compared to them, in line with the
5 observations performed in previous studies (Chaud et al., 2021). The result suggests the possibility
6 to reduce the amount of insecticide to control target insect pests with no decrease in efficacy, with
7 an advantage for the environment. Wax moth larvae were more susceptible than yellow mealworm
8 adults. It is, however, well-known that the latter are not very sensitive to pyrethrins (Pedersen et al.,
9 2020), thus they can be used to evaluate the performances of the nanomaterial synthesized on
10 different pests with a different sensibility to the treatment. Therefore, the controlled release
11 nanoformulation described in this work has great potential in the development of low-cost and
12 environmentally friendly formulations of botanical insecticides for sustainable pest control.

13 **Acknowledgments**

14 The authors are thankful to Dr. Emma Lambert.

15 **5. References**

- 16 Abdullayev, E., Lvov, Y., 2011. Halloysite Clay Nanotubes for Controlled Release of Protective Agents.
17 Journal of Nanoscience and Nanotechnology 11, 10007-10026.
- 18 Ahmad, R., Hussein, M.Z., Wan Abdul Kadir, W.R., Sarijo, S.H., Yun Hin, T.-Y., 2015. Evaluation of Controlled-
19 Release Property and Phytotoxicity Effect of Insect Pheromone Zinc-Layered Hydroxide Nanohybrid
20 Intercalated with Hexenoic Acid. J. Agric. Food. Chem. 63, 10893-10902.
- 21 Ahmed, F.R., Shoaib, M.H., Azhar, M., Um, S.H., Yousuf, R.I., Hashmi, S., Dar, A., 2015. In-vitro assessment
22 of cytotoxicity of halloysite nanotubes against HepG2, HCT116 and human peripheral blood lymphocytes.
23 Colloids and Surfaces B: Biointerfaces 135, 50-55.
- 24 Bellani, L., Giorgetti, L., Riela, S., Lazzara, G., Scialabba, A., Massaro, M., 2016. Ecotoxicity of halloysite
25 nanotube-supported palladium nanoparticles in *Raphanus sativus* L. Environ. Toxicol. Chem. 35, 2503-
26 2510.
- 27 Bombo, A.B., Pereira, A.E.S., Lusa, M.G., de Medeiros Oliveira, E., de Oliveira, J.L., Campos, E.V.R., de Jesus,
28 M.B., Oliveira, H.C., Fraceto, L.F., Mayer, J.L.S., 2019. A Mechanistic View of Interactions of a Nanoherbicide
29 with Target Organism. J. Agric. Food. Chem. 67, 4453-4462.
- 30 Bretti, C., Cataldo, S., Gianguzza, A., Lando, G., Lazzara, G., Pettignano, A., Sammartano, S., 2016.
31 Thermodynamics of Proton Binding of Halloysite Nanotubes. The Journal of Physical Chemistry C 120, 7849-
32 7859.
- 33 Cavallaro, G., Milioto, S., Konnova, S., Fakhrullina, G., Akhatova, F., Lazzara, G., Fakhrullin, R., Lvov, Y., 2020.
34 Halloysite/Keratin Nanocomposite for Human Hair Photoprotection Coating. ACS Appl. Mater. Interf. 12,
35 24348-24362.

1 Chaud, M., Souto, E.B., Zielinska, A., Severino, P., Batain, F., Oliveira-Junior, J., Alves, T., 2021.
2 Nanopesticides in Agriculture: Benefits and Challenge in Agricultural Productivity, Toxicological Risks to
3 Human Health and Environment. *Toxics* 9, 131.

4 Chen, L., Guo, Z., Lao, B., Li, C., Zhu, J., Yu, R., Liu, M., 2021a. Phytotoxicity of halloysite nanotubes using
5 wheat as a model: seed germination and growth. *Environm. Sci. Nano*.

6 Chen, L., Guo, Z., Lao, B., Li, C., Zhu, J., Yu, R., Liu, M., 2021b. Phytotoxicity of halloysite nanotubes using
7 wheat as a model: seed germination and growth. *Environmental Science: Nano* 8, 3015-3027.

8 Chen, L., Huang, J., Chen, J., Shi, Q., Chen, T., Qi, G., Liu, M., 2022. Halloysite Nanotube-Based Pesticide
9 Formulations with Enhanced Rain Erosion Resistance, Foliar Adhesion, and Insecticidal Effect. *ACS Applied*
10 *Materials and Interfaces*.

11 Chrustek, A., Hołyńska-Iwan, I., Dziembowska, I., Bogusiewicz, J., Wróblewski, M., Cwynar, A., Olszewska-
12 Słonina, D., 2018. Current Research on the Safety of Pyrethroids Used as Insecticides. *Medicina (Kaunas)* 54,
13 61.

14 Crombie, L., 1999. Natural product chemistry and its part in the defence against insects and fungi in
15 agriculture†. *Pestic. Sci.* 55, 761-774.

16 da Rocha, M.C., Braz, E.M.d.A., Honório, L.M.C., Trigueiro, P., Fonseca, M.G., Silva-Filho, E.C., Carrasco,
17 S.M., Polo, M.S., Iborra, C.V., Osajima, J.A., 2019. Understanding the effect of UV light in systems containing
18 clay minerals and tetracycline. *Applied Clay Science* 183, 105311.

19 da Rocha, M.C., Galdino, T., Trigueiro, P., Honorio, L.M.C., de Melo Barbosa, R., Carrasco, S.M., Silva-Filho,
20 E.C., Osajima, J.A., Viseras, C., 2022. Clays as Vehicles for Drug Photostability. *Pharmaceutics* 14, 796.

21 de Oliveira, L.H., Trigueiro, P., Souza, J.S.N., de Carvalho, M.S., Osajima, J.A., da Silva-Filho, E.C., Fonseca,
22 M.G., 2022. Montmorillonite with essential oils as antimicrobial agents, packaging, repellents, and
23 insecticides: an overview. *Colloids Surf. B. Biointerfaces* 209, 112186.

24 Dindo, M.L., Marchetti, E., Galvagni, G., Baronio, P., 2003. Rearing of *Exorista larvarum* (Diptera
25 Tachinidae): simplification of the in vitro technique.

26 Fakhrullina, G.I., Akhatova, F.S., Lvov, Y.M., Fakhrullin, R.F., 2015. Toxicity of halloysite clay nanotubes in
27 vivo: a *Caenorhabditis elegans* study. *Environm. Sci. Nano* 2, 54-59.

28 Ghezzi, L., Spepi, A., Agnolucci, M., Cristani, C., Giovannetti, M., Tiné, M.R., Duce, C., 2018. Kinetics of
29 release and antibacterial activity of salicylic acid loaded into halloysite nanotubes. *Applied Clay Science* 160,
30 88-94.

31 Glotov, A., Vutolkina, A., Pimerzin, A., Vinokurov, V., Lvov, Y., 2021. Clay nanotube-metal core/shell
32 catalysts for hydroprocesses. *Chem. Soc. Rev.* 50, 9240-9277.

33 Gomez-Zavaglia, A., Mejuto, J.C., Simal-Gandara, J., 2020. Mitigation of emerging implications of climate
34 change on food production systems. *Food Res. Int.* 134, 109256.

35 Hasani, M., Abdouss, M., Shojaei, S., 2021. Nanocontainers for drug delivery systems: A review of Halloysite
36 nanotubes and their properties. *International Journal of Artificial Organs* 44, 426-433.

37 Head, S.W., 1973. Chapter 3 - Composition of Pyrethrum Extract and Analysis of Pyrethrins, in: Casida, J.E.
38 (Ed.), *Pyrethrum*. Academic Press, pp. 25-53.

39 Hill, D.S., 1990. *Pests of Stored Foodstuffs and Their Control*. Kluwer Academic Publishers.

40 Huang, X., Huang, Y., Wang, D., Liu, M., Li, J., Chen, D., 2021. Cellular response of freshwater algae to
41 halloysite nanotubes: alteration of oxidative stress and membrane function. *Environmental Science: Nano*
42 8, 3262-3272.

43 Ignasiak, K., Maxwell, A., 2017. *Galleria mellonella* (greater wax moth) larvae as a model for antibiotic
44 susceptibility testing and acute toxicity trials. *BMC Research Notes* 10, 428.

45 Jeran, N., Grdiša, M., Varga, F., Šatović, Z., Liber, Z., Dabić, D., Biošić, M., 2021. Pyrethrin from Dalmatian
46 pyrethrum (*Tanacetum cinerariifolium* (Trevir.) Sch. Bip.): biosynthesis, biological activity, methods of
47 extraction and determination. *Phytochem. Rev.* 20, 875-905.

48 JOUSSEIN, E., PETIT, S., CHURCHMAN, J., THENG, B., RIGHI, D., DELVAUX, B., 2005. Halloysite clay minerals
49 — a review. *Clay Minerals* 40, 383-426.

50 Kah, M., Kookana, R.S., Gogos, A., Bucheli, T.D., 2018. A critical evaluation of nanopesticides and
51 nanofertilizers against their conventional analogues. *Nat. Nanotechnol.* 13, 677-684.

- 1 Kalaitzaki, A., Papanikolaou, N.E., Karamaouna, F., Dourtoglou, V., Xenakis, A., Papadimitriou, V., 2015.
2 Biocompatible Colloidal Dispersions as Potential Formulations of Natural Pyrethrins: A Structural and
3 Efficacy Study. *Langmuir* 31, 5722-5730.
- 4 Kawamoto, M., Moriyama, M., Ashida, Y., Matsuo, N., Tanabe, Y., 2020. Total Syntheses of All Six Chiral
5 Natural Pyrethrins: Accurate Determination of the Physical Properties, Their Insecticidal Activities, and
6 Evaluation of Synthetic Methods. *J. Org. Chem.* 85, 2984-2999.
- 7 Kay, S., Edwards, J., Brown, J., Dixon, R., 2019. *Galleria mellonella* Infection Model Identifies Both High and
8 Low Lethality of *Clostridium perfringens* Toxigenic Strains and Their Response to Antimicrobials. *Front.*
9 *Microbiol.* 10.
- 10 Kaya, S., 2020. THE EFFECTS OF PYRETHRUM EXTRACT ON *Galleria mellonella* HEMOLYMPH
11 PHENOLOXIDASE ENZYME. *HEALTH SCIENCES QUARTERLY* 4, 269-280.
- 12 Kogure, T., 2016. Chapter 5 - Characterisation of Halloysite by Electron Microscopy, in: Yuan, P., Thill, A.,
13 Bergaya, F. (Eds.), *Developments in Clay Science*. Elsevier, pp. 92-114.
- 14 Kwadha, C.A., Ong'amo, G.O., Ndegwa, P.N., Raina, S.K., Fombong, A.T., 2017. The Biology and Control of
15 the Greater Wax Moth, *Galleria mellonella*. *Insects* 8, 61.
- 16 Li, X., Wen, Y., Zhang, Y., Ge, Z., 2022. Pheromone enclosed in halloysite with n-octadecane releases
17 rhythmically under simulated diurnal temperature. *Applied Clay Science* 217, 106386.
- 18 Lisuzzo, L., Cavallaro, G., Milioto, S., Lazzara, G., 2020. Halloysite Nanotubes Coated by Chitosan for the
19 Controlled Release of Khellin. *Polymers* 12, 1766.
- 20 Lisuzzo, L., Cavallaro, G., Pasbakhsh, P., Milioto, S., Lazzara, G., 2019. Why does vacuum drive to the loading
21 of halloysite nanotubes? The key role of water confinement. *J. Colloid Interface Sci.* 547, 361-369.
- 22 Long, Y., Feng, Y., He, Y., Luo, B., Liu, M., 2022. Hyaluronic Acid Modified Halloysite Nanotubes Decorated
23 with ZIF-8 Nanoparticles as Dual Chemo- and Photothermal Anticancer Agents. *ACS Appl. Nano Mater.* 5,
24 5813-5825.
- 25 Long, Z., Wu, Y.-P., Gao, H.-Y., Zhang, J., Ou, X., He, R.-R., Liu, M., 2018. In vitro and in vivo toxicity
26 evaluation of halloysite nanotubes. *Journal of Materials Chemistry B* 6, 7204-7216.
- 27 Marchetti, E., Alberghini, S., Battisti, A., Squartini, A., Baronio, P., Dindo, M.L., 2009. Effects of conventional
28 and transgenic *Bacillus thuringiensis galleriae* toxin on *Exorista larvarum* (Diptera: Tachinidae), a parasitoid
29 of forest defoliating Lepidoptera. *Biocontrol Sci. Technol.* 19, 463-473.
- 30 Markham, T.E., Kotze, A.C., Duggan, P.J., Johnston, M.R., 2021. Reduction Chemistry of Natural Pyrethrins
31 and Preliminary Insecticidal Activity of Reduced Pyrethrins. *Aust. J. Chem.* 74, 268-281.
- 32 Martin, S.J., 2004. Acaricide (pyrethroid) resistance in *Varroa destructor*. *Bee World* 85, 67-69.
- 33 Massaro, M., Colletti, C.G., Buscemi, G., Cataldo, S., Guernelli, S., Lazzara, G., Liotta, L.F., Parisi, F.,
34 Pettignano, A., Riela, S., 2018. Palladium nanoparticles immobilized on halloysite nanotubes covered by a
35 multilayer network for catalytic applications. *New J. Chem.* 42, 13938-13947.
- 36 Massaro, M., Licandro, E., Cauteruccio, S., Lazzara, G., Liotta, L.F., Notarbartolo, M., Raymo, F.M., Sánchez-
37 Espejo, R., Viseras-Iborra, C., Riela, S., 2022a. Nanocarrier based on halloysite and fluorescent probe for
38 intracellular delivery of peptide nucleic acids. *J. Colloid Interface Sci.* 620, 221-233.
- 39 Massaro, M., Notarbartolo, M., Raymo, F.M., Cavallaro, G., Lazzara, G., Mazza, M.M.A., Viseras-Iborra, C.,
40 Riela, S., 2022b. Supramolecular Association of Halochromic Switches and Halloysite Nanotubes in
41 Fluorescent Nanoprobes for Tumor Detection. *ACS Appl. Nano Mater.*
- 42 Massaro, M., Noto, R., Riela, S., 2020. Past, present and future perspectives on halloysite clay minerals.
43 *Molecules* 25.
- 44 MOSTELLER, F., YOUTZ, C., 1961. Tables of the Freeman-Tukey transformations for the binomial and
45 Poisson distributions*. *Biometrika* 48, 433-440.
- 46 Pajnik, J., Radetić, M., Stojanovic, D.B., Jankovic-Častvan, I., Tadic, V., Stanković, M.V., Jovanović, D.M.,
47 Zizovic, I., 2018. Functionalization of polypropylene, polyamide and cellulose acetate materials with
48 pyrethrum extract as a natural repellent in supercritical carbon dioxide. *The Journal of Supercritical Fluids*
49 136, 70-81.
- 50 Papanikolaou, N.E., Kalaitzaki, A., Karamaouna, F., Michaelakis, A., Papadimitriou, V., Dourtoglou, V.,
51 Papachristos, D.P., 2018. Nano-formulation enhances insecticidal activity of natural pyrethrins against *Aphis*
52 *gossypii* (Hemiptera: Aphididae) and retains their harmless effect to non-target predators. *Environm. Sci.*
53 *Poll. Res.* 25, 10243-10249.

1 Pedersen, K.E., Pedersen, N.N., Meyling, N.V., Fredensborg, B.L., Cedergreen, N., 2020. Differences in life
2 stage sensitivity of the beetle *Tenebrio molitor* towards a pyrethroid insecticide explained by stage-specific
3 variations in uptake, elimination and activity of detoxifying enzymes. *Pestic. Biochem. Physiol.* 162, 113-
4 121.

5 Praveen, B., Sharma, P., 2019. A review of literature on climate change and its impacts on agriculture
6 productivity. *Journal of Public Affairs* 19, e1960.

7 Prinz Setter, O., Segal, E., 2020. Halloysite nanotubes – the nano-bio interface. *Nanoscale* 12, 23444-23460.

8 Qin, Y., An, T., Cheng, H., Su, W., Meng, G., Wu, J., Guo, X., Liu, Z., 2022. Functionalized halloysite
9 nanotubes as chlorpyrifos carriers with high adhesion and temperature response for controlling of beet
10 armyworm. *Applied Clay Science* 222, 106488.

11 R. Price, B.P.G.Y.L.R., 2001. In-vitro release characteristics of tetracycline HCl, khellin and nicotinamide
12 adenine dinucleotide from halloysite; a cylindrical mineral. *J. Microencapsulation* 18, 713-722.

13 Riela, S., Barattucci, A., Barreca, D., Campagna, S., Cavallaro, G., Lazzara, G., Massaro, M., Pizzolanti, G.,
14 Salerno, T.M.G., Bonaccorsi, P., Puntoriero, F., 2021. Boosting the properties of a fluorescent dye by
15 encapsulation into halloysite nanotubes. *Dyes and Pigments* 187.

16 Santos, A.C., Ferreira, C., Veiga, F., Ribeiro, A.J., Panchal, A., Lvov, Y., Agarwal, A., 2018. Halloysite clay
17 nanotubes for life sciences applications: From drug encapsulation to bioscaffold. *Adv. Colloid Interface Sci.*
18 257, 58-70.

19 Saucedo-Zuñiga, J.N., Sánchez-Valdes, S., Ramírez-Vargas, E., Guillen, L., Ramos-deValle, L.F., Graciano-
20 Verdugo, A., Uribe-Calderón, J.A., Valera-Zaragoza, M., Lozano-Ramírez, T., Rodríguez-González, J.A.,
21 Borjas-Ramos, J.J., Zuluaga-Parra, J.D., 2021. Controlled release of essential oils using laminar nanoclay and
22 porous halloysite / essential oil composites in a multilayer film reservoir. *Microporous Mesoporous Mater.*
23 316, 110882.

24 Shao, C., Zhao, H., Wang, P., 2022. Recent development in functional nanomaterials for sustainable and
25 smart agricultural chemical technologies. *Nano Convergence* 9, 11.

26 Soderlund, D.M., 2010. Chapter 77 - Toxicology and Mode of Action of Pyrethroid Insecticides, in: Krieger,
27 R. (Ed.), *Hayes' Handbook of Pesticide Toxicology* (Third Edition). Academic Press, New York, pp. 1665-1686.

28 Wang, X., Gong, J., Rong, R., Gui, Z., Hu, T., Xu, X., 2018. Halloysite Nanotubes-Induced Al Accumulation and
29 Fibrotic Response in Lung of Mice after 30-Day Repeated Oral Administration. *Journal of Agricultural and*
30 *Food Chemistry* 66, 2925-2933.

31 Wibowo, D., Zhao, C.-X., Peters, B.C., Middelberg, A.P.J., 2014. Sustained Release of Fipronil Insecticide in
32 Vitro and in Vivo from Biocompatible Silica Nanocapsules. *J. Agric. Food. Chem.* 62, 12504-12511.

33 Yan, S., Hu, Q., Li, J., Chao, Z., Cai, C., Yin, M., Du, X., Shen, J., 2019. A Star Polycation Acts as a Drug
34 Nanocarrier to Improve the Toxicity and Persistence of Botanical Pesticides. *ACS Sustainable Chemistry &*
35 *Engineering* 7, 17406-17413.

36 Zhai, Y., Abdolapur Monikh, F., Wu, J., Grillo, R., Arenas-Lago, D., Darbha, G.K., Vijver, M.G., Peijnenburg,
37 W.J.G.M., 2020. Interaction between a nano-formulation of atrazine and rhizosphere bacterial
38 communities: atrazine degradation and bacterial community alterations. *Environm. Sci. Nano* 7, 3372-3384.

39 Zhang, Y., Chen, W., Jing, M., Liu, S., Feng, J., Wu, H., Zhou, Y., Zhang, X., Ma, Z., 2019. Self-assembled mixed
40 micelle loaded with natural pyrethrins as an intelligent nano-insecticide with a novel temperature-
41 responsive release mode. *Chem. Eng. J.* 361, 1381-1391.

42 Zhong, B., Wang, S., Dong, H., Luo, Y., Jia, Z., Zhou, X., Chen, M., Xie, D., Jia, D., 2017. Halloysite Tubes as
43 Nanocontainers for Herbicide and Its Controlled Release in Biodegradable Poly(vinyl alcohol)/Starch Film. *J.*
44 *Agric. Food. Chem.* 65, 10445-10451.